Dynamics of glass-forming liquids. XVII. Dielectric relaxation and intermolecular association in a series of isomeric octyl alcohols

ARTICLE *in* THE JOURNAL OF CHEMICAL PHYSICS · OCTOBER 2013

Impact Factor: 2.95 · DOI: 10.1063/1.4823998 · Source: PubMed

3 AUTHORS, INCLUDING:

Lokendra P. Singh
University of Claude Bernard Lyon 1, Villeurb…

13 PUBLICATIONS **114** CITATIONS

SEE PROFILE

Dynamics of glass-forming liquids. XVII. Dielectric relaxation and intermolecular association in a series of isomeric octyl alcohols

Lokendra P. Singh,[1] Christiane Alba-Simionesco,[2] and Ranko Richert[1]
[1]*Department of Chemistry and Biochemistry, Arizona State University, Tempe, Arizona 85287-1604, USA*
[2]*Laboratoire Léon Brillouin, CNRS /CEA -UMR 12, DSM/IRAMIS/LLB CEA Saclay, 91191 Gif-sur-Yvette Cedex, France*

(Received 18 July 2013; accepted 18 September 2013; published online XX XX XXXX)

It is well established that many mono-hydroxy alcohols show an extra relaxation process of the Debye type in addition to the signatures of primary and secondary structural relaxations, which is observed only in dielectric spectroscopy and related techniques. In order to gain further insight into the nature of this Debye peak, we study the linear and nonlinear dielectric behavior of a series of isomeric octyl alcohols and of mixtures of *n*-propanol with one of the octanols. These samples display systematic variations of the Debye peak intensity and concomitant changes in the Kirkwood correlation factor g_K from 0.1 to 4, indicative of different equilibrium constants, $K_{c/r}$, that characterize the populations of non-polar ring and polar open chain structures. For cases where $K_{c/r}$ is not too far from unity, we find that a high electric field shifts $K_{c/r}$ towards more chains, and that the accompanying change in the end-to-end vector of hydrogen-bond connected structures occurs on the Debye time scale. The results suggest that g_K is correlated with the spectral separation of the Debye and primary structural peaks, as both features depend on steric hindrance of chain flexibility or bond rotation barriers and on average chain lengths. Based on the complex dynamics of supercooled mono-hydroxy alcohols with three relaxation peaks that cover many orders of magnitude in frequency, it is argued that a frequency dependent g_K may be required for assessing the average orientational correlations within hydrogen-bonded structures correctly. © *2013 AIP Publishing LLC*. [http://dx.doi.org/10.1063/1.4823998]

I. INTRODUCTION

Hydrogen bonds play an essential role regarding the properties of liquids such as water, alcohols, and amides. These intermolecular interactions are also an important feature of more viscous and solid materials such as sugar solutions, foods, and biological systems. In the majority of hydrogen-bonding cases, a hydroxyl group is involved, which is associated with a significant dipole moment of about 1.7 D.[1] Consequently, dielectric techniques have been employed extensively with the aim of elucidating the structure and dynamics of hydrogen-bonded materials.[2,3] Numerous alcohols have been the subject of dielectric relaxation studies, and in many cases the most prominent dielectric polarization process is found to obey a Debye type (single exponential, non-dispersive) relaxation behavior. Such an observation is particularly noteworthy in the case of glass-forming alcohols in their viscous state, where Debye type processes are an exception.[4,5]

When a liquid is cooled sufficiently fast to below its melting temperature T_m, crystallization can be avoided and the characteristic relaxation times in this supercooled regime increase rapidly upon cooling. Near the glass transition temperature, T_g, the time scales associated with structural rearrangements exceed typical experimental time scales, e.g., $\tau_g(T_g) = 100$ s, and the material enters a non-equilibrium glassy solid state.[6] For determining the relaxation dynamics of supercooled liquids, broadband dielectric spectroscopy is used extensively because of its high sensitivity and capability of covering an extremely broad dynamic range as compared to most other spectroscopic methods.[7] Typical molecular glass-formers display some very general features: They exhibit multiple non-exponential relaxation processes, with the main and usually slowest process referred to as α-process or primary structural relaxation.[8] This non-exponential primary relaxation process is well represented by the Kohlrausch-Williams-Watts (KWW)[9,10] response function in the time domain given by $\Phi(t) = \Phi_0 \exp[-(t/\tau)^{\beta_{KWW}}]$. Here, $0 < \beta_{KWW} \leq 1$, gauges the extent of the relaxation time dispersion, and for typical viscous liquids the value of β_{KWW} is considerably below the Debye limit represented by $\beta_{KWW} = 1$. Moreover, the relaxation times corresponding to this α-process usually follow a Vogel-Fulcher-Tammann (VFT) type temperature dependence over several decades in time,[11–13] which is given by

$$\log_{10}[\tau(T)/s] = A + \frac{B}{T - T_0}. \quad (1)$$

In this expression, T_0 is the temperature at which the dynamics of the system tends to diverge, A is a logarithmic pre-exponential factor, and B is a constant activation parameter. In addition to the primary structural process described above, further higher frequency processes can also be observed in many glass forming materials. Examples are the so-called Johari-Goldstein β-relaxation (β_{JG}) and γ-processes.[14] These secondary relaxations are considered to reflect more localized motions and usually follow an Arrhenius type temperature dependence, i.e., Eq. (1) with $T_0 = 0$.

The relaxation dynamics of most supercooled mono-hydroxy alcohols do not follow the above pattern typical of molecular liquids.[4,5,15,16] Instead, the dielectric loss spectra of many mono-hydroxy alcohols show a Debye type relaxation process as their most prominent and lowest frequency loss peak, which follows a VFT temperature dependence with $T_0 \gg 0$. In contrast to simple liquids, this dominant low frequency process is not the immediate signature of structural relaxation, as demonstrated by comparing the dielectric features with mechanical,[17,18] specific heat,[19–21] light scattering,[5] nuclear magnetic resonance,[22,23] as well as physical aging results.[24] These measurements clearly show that the process responsible for the dielectric Debye signal does not contribute to mechanical, enthalpy, or structural relaxation modes in an obvious manner. Several phenomenological and theoretical models aimed at explaining the Debye model have been discussed,[25–28] but a generally accepted picture of the molecular origin of this process had not evolved during the initial decades of research on this topic.

The above features described for the case of mono-hydroxy alcohols do not occur in every liquid that involves hydrogen-bonding. For example, such a dielectric Debye peak is not found in most polyalcohols or diols.[29–31] Moreover, it has been observed that some mono-hydroxy alcohols can lack this Debye process, e.g., salol, 2-phenyl-1-ethanol,[4] 1-phenyl-1-propanol,[32] and 1-phenyl-2-propanol.[33] The explanations of these exceptions are based on steric hindrances that prevents the capability of forming an intermolecular hydrogen-bonded network.[34,35] Therefore, molecular structure has a considerable impact on the dielectric properties of alcohols.[36]

In 1968, Dannhauser had reported the consequence of the molecular structure of isomeric octyl alcohols on the static dielectric constant[34] and on the dynamics.[37] He showed by a systematic variation of the methyl group ($–CH_3$) position relative to the fixed location of the hydroxyl group (–OH), that the value of the static dielectric constant increases with increasing separation between the –OH and $–CH_3$ groups. Because the gas state dipole moment of isomeric octanols is practically independent of the methyl group position, the variation in the static permittivity has to reflect the substantial differences in the structure of liquids and the concomitant orientational correlation of permanent dipoles, as gauged by the Kirkwood correlation factor g_K.[2,38] Dannhauser[34,37] concluded that an increased steric hindrance of hydroxyl chain formation alters the predominant structure of hydrogen-bonded molecules from chain to ring like structures, accompanied by a reduction in the dielectric constant and g_K, as well as the gradual disappearance of the Debye peak. Accordingly, this series of isomers provides excellent examples for studying the nature of the prominent dielectric Debye process of mono-hydroxy alcohols.

In order to investigate the correlation between the structure and dynamics of hydrogen-bonded liquids and the molecular structure of its constituents, we have critically examined the dielectric behavior of glass forming mono-hydroxy alcohols at low and at high electric fields using broadband dielectric spectroscopy. The liquids investigated are four isomeric octanols, 3-methyl-3-heptanol (3M3H), 4-methyl-3-heptanol (4M3H), 5-methyl-3-heptanol (5M3H), and 6-methyl-3-heptanol (6M3H), as well as mixtures of *n*-propanol (*n*POH) with 4-methyl-3-heptanol. Adding *n*-propanol to 4-methyl-3-heptanol allows us to gradually reduce the steric hindrance to chain formation and thus increase the value of g_K by adjusting composition, similar to the methyl group position effect in the series of octanols. For all systems, the signatures of both primary and secondary structural relaxation can be identified. Additionally, an extra dielectric Debye peak is observed, the magnitude of which depends strongly on the –OH to $–CH_3$ distance and on the composition of the propanol/octanol mixture. Whenever the chain-to-ring structure equilibrium constant, $K_{c/r}$, is not too far from unity, the chain population can be enhanced by a high electric field. The time scale of the field induced chain formation is twice the dielectric Debye time, τ_D, for all cases. The present results strongly support a recent model of the Debye process based on a high field dielectric study of 5-methyl-3-heptanol,[39] where the process is assumed to originate from the end-to-end vector fluctuations of hydrogen-bonded chain like structures.

II. EXPERIMENT

The chemicals used in this study are 3M3H, 4M3H, 5M3H, 6M3H, and nPOH. All these liquids were purchased from Sigma-Aldrich and used as received. The stated purities are $\geq$ 99% for 4M3H and 99.7% (anhydrous) for nPOH, while no purity levels were specified for the other liquids.

The linear-response dielectric measurements are performed by holding the liquid between two brass electrodes (lower electrode of 30 mm diameter and an upper electrode of 20 mm diameter) which are separated by thin Teflon strips arranged in a radial geometry. The dimensions of this capacitor with 20 mm diameter and 50 μm thickness result in a geometric capacity of $C_0 = 55.6$ pF. All samples are measured inside a nitrogen-gas cryostat where the temperature is stabilized and measured by a Novocontrol Quatro controller, with a stability of the temperature reading better than 0.05 K. Frequency dependent impedance measurements were performed using a Solartron SI-1260 gain-phase analyzer equipped with a Mestec DM-1360 transimpedance amplifier. Data are acquired for frequencies in the range $10^{-2} \leq \nu \leq 10^6$ Hz, with the frequencies being logarithmically spaced at a density of 8 per decade. Before introducing the sample material into the cell, a reference measurement is performed at room temperature in order to calibrate the transimpedance of the current sensing amplifier.

In addition, some samples were also measured in a higher frequency range, 1 MHz-2 GHz, using a Novocontrol high frequency dielectric spectrometer based upon the Agilent radio frequency impedance analyzer 4192B. Prior to the sample measurement, basic calibrations were performed using the following terminators: open, short, 50 Ω load, and a low loss capacitor standard. For each of the terminators, the calibration is carried out automatically by the Novocontrol software. For the actual measurement, the sample was placed between parallel gold plated electrodes of 10 mm diameter and 90 μm electrode separation as defined by an annular Teflon spacer. When necessary, the overall amplitude resulting from

such a higher frequency scan was adjusted to the low frequency results on the basis of the overlapping frequency range (1-10 MHz).

High-field impedance data for frequencies between 0.1 Hz and 100 kHz are acquired using the SI-1260 gain/phase analyzer, with the voltage output amplified by a factor of 100 via a Trek Model PZD-350 high-voltage amplifier and connected to the "high potential" side of the sample capacitor. That potential is measured via the voltage monitor signal (1 V/100 V) of the PZD-350 which is routed into the "V_1" input of the SI-1260. The "low potential" side of the capacitor is connected to ground via a shunt of impedance Z_s, realized by a network of four resistors and four capacitors. The increase of the impedance Z_s from about 10 Ω at 100 kHz towards saturating at 1 MΩ below 1 Hz helps to counteract the reduction of the voltage across the shunt when the current becomes very small at the low frequencies. The voltage drop across this shunt is fed into a home built linear buffer amplifier ($V_{out} = V_{in}$ for frequencies $\nu < 800$ kHz) that sustains 500 V_p at the input and thus protects the SI-1260 against sample failure. The output of this amplifier gauges the current through the sample and is connected to the "V_2" input of the SI-1260. For a given set of frequencies, the analyzer determines the sample impedance from the voltage across the capacitor ($V_1 - V_2$) and the current through the sample (V_2/Z_s). At each frequency, a measurement at the higher field is followed by two low field measurements, with the first low field measurement acting only as recovery time for the sample. At each frequency ν, the delay and integration times of the SI-1260 are set to $3/\nu$ and $6/\nu$, respectively, but with a minimum duration of 10 ms. The shunt and both amplifiers are calibrated using a 100 pF loss free ($\tan\delta < 6 \times 10^{-5}$) polystyrene capacitor. For the sample measurement, the stainless steel electrodes are spaced 10 μm apart with an annular Teflon spacer that leaves a free inner diameter of 14 mm for the sample. The added capacitance originating from the Teflon surface within the active electrode area has been subtracted from all data. The loaded cell is cooled in a Novocontrol Quatro liquid-nitrogen cryostat system.

Differential scanning calorimetry (DSC) results were obtained employing a TA-Instrument Model Q100 in standard mode. DSC measurements were performed with both cooling and heating rates set to 10 K/min. Hermetically sealed aluminum pans were used for all liquid samples. The masses of the samples amounted to about 12.5 mg. In order to see the thermal behavior of isomeric octanols, first the liquid samples were cooled at a rate of 10 K/min to the lowest temperature, i.e., 130 K. Subsequently, the data were collected by heating the sample at a rate of 10 K/min from 130 to 270 K. The DSC instrument was temperature calibrated at the rates of ± 10 K/min using Indium as standard.

III. RESULTS

In order to analyze the dielectric relaxation results, $\varepsilon^*(\omega) = \varepsilon'(\omega) - i\varepsilon''(\omega)$, the following frequency domain expression is employed to fit the spectra, which is based upon the Havriliak-Negami (HN) function and special cases thereof.[40] Following common practice, the entire loss spectrum is fit by the sum of three processes plus dc-conductivity:

$$\varepsilon^*(\omega) = \varepsilon_\infty + \frac{\Delta\varepsilon_D}{1 + i\omega\tau_D} + \frac{\Delta\varepsilon_\alpha}{\left[1 + (i\omega\tau_\alpha)^\alpha\right]^\gamma} + \frac{\Delta\varepsilon_\beta}{1 + (i\omega\tau_\beta)^\beta} + \frac{\sigma_{dc}}{i\omega\varepsilon_0}. \quad (2)$$

Here, each process is characterized by its relaxation strength $\Delta\varepsilon$, its relaxation time constant τ, and the shape parameters, α, γ, and β, which determine the broadening and asymmetry of the loss curve with $0 < \alpha, \alpha\gamma, \beta \leq 1$. The overall high frequency limit of the real part of the permittivity is denoted ε_∞, and the static dielectric constant is $\varepsilon_s = \varepsilon_\infty + \Delta\varepsilon_D + \Delta\varepsilon_\alpha + \Delta\varepsilon_\beta$. In the present case, a Debye function was used to fit the lowest frequency Debye peak (D-process), a HN-function is employed to fit the primary structural mode (α-process), and a Cole-Cole function for the secondary relaxation (β-process), listed in the order of increasing peak frequency.

A. Isomeric octyl alcohols: Low field

The low field limit dielectric spectra of the four methylated heptanols, 3M3H, 4M3H, 5M3H, and 6M3H, are presented in Fig. 1. These results are consistent with dielectric relaxation data published previously for these liquids.[4,34,41] Although the compounds differ only in the methyl group position, the appearances of the temperature dependent spectra differ considerably. While only a dispersive low amplitude loss peak is seen in the case of highly viscous 3M3H, an additional lower frequency Debye peak appears in the case of 4M3H, and for 5M3H and 6M3H the spectra are dominated by the Debye process. Another obvious difference is the trend of the relaxation amplitude with increasing temperature. In order to characterize the dielectric behavior in more detail, the results were fit using Eq. (2).

Representative fit results for the octanol analysis are shown for 4M3H and 6M3H in Fig. 2. The activation traces

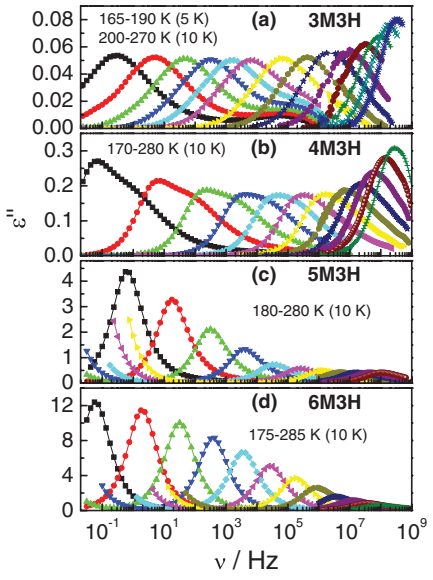

FIG. 1. Dielectric loss spectra of four isomeric octyl alcohols for the temperatures indicated: (a) 3M3H, (b) 4M3H, (c) 5M3H, and (d) 6M3H.

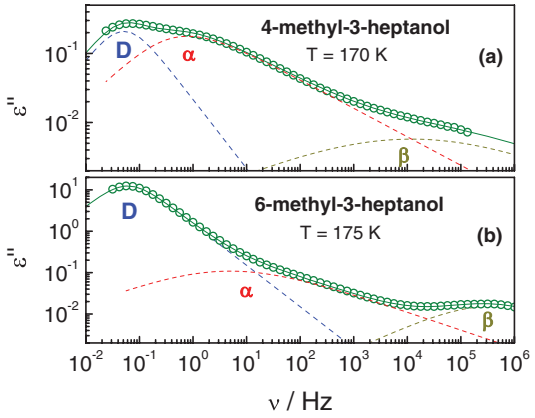

FIG. 2. Representative fits to the dielectric loss spectra showing the three distinct contributions as dashed lines labeled "D," "α," and "β," as well as the total fit shown as solid line. The cases shown are for: (a) 4M3H at $T = 170$ K, and (b) 6M3H at $T = 175$ K.

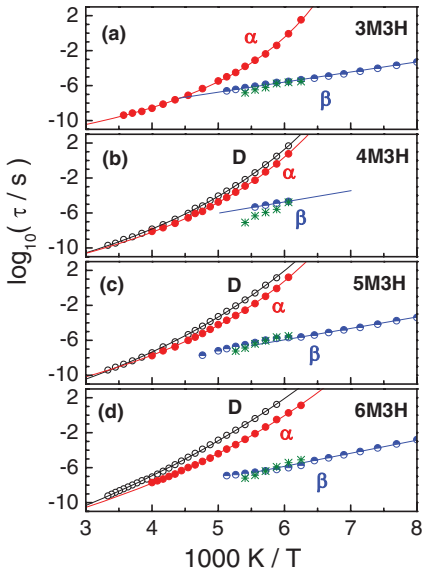

FIG. 3. Activation plot of the time constants τ_D, τ_α, and τ_β for four isomeric octyl alcohols. Round symbols represent the experimental fit parameter results, while the solid lines are for the VFT fits using the parameters listed in Table I. The stars are coupling model predictions for the JG type secondary process according to Eq. (5). The different panels are for (a) 3M3H, (b) 4M3H, (c) 5M3H, and (d) 6M3H.

resulting from all fits are compiled in Fig. 3, showing three distinct relaxation processes in each case except for 3M3H, in which case a separate Debye process could not be discerned. All four compounds show a dispersive relaxation peak with VFT type temperature dependence of the characteristic time constant which is identified as the signature of the primary structural mode (α). All isomers also display a secondary structural process with Cole-Cole type dispersion and Arrhenius temperature dependence (β). Additional slower Debye peaks are observed for all octanols except 3M3H, and these Debye type loss peaks are subject to VFT temperature dependences that are similar to those of the respective α-peaks. However, the spectral separation of the Debye and α-process does change with temperature. The fit parameters characterizing the curves in Fig. 3 are compiled in Table I.

The static dielectric constants, ε_s, for all four isomers are derived from the low frequency values of $\varepsilon'(\omega)$, where a plateau across at least a decade of frequency between 0.1 Hz and 1 MHz is observed, without interference of electrode polarization. The results for ε_s are depicted in Fig. 4, demonstrating more clearly than in Fig. 1 that the effect of temperature on ε_s differs qualitatively for the different isomers. None of the $\varepsilon_s(T)$ curves can be explained solely on the basis of the Boltzmann term that reduces the dielectric constant approximately as $1/T$ with increasing temperature. The DSC traces of 3M3H, 4M3H, and 5M3H shown in Fig. 5 indicate that the calorimetric glass transition temperatures, T_g, are within a few Kelvin of one another for the three isomers investigated. The origin of the extra feature near 175 K for 3M3H is unclear.

B. Mixture with propanol: Low field

For the mixtures of nPOH in 4M3H, it was found that up to a mole fraction of nPOH of $x = 0.20$, the binary system is a completely transparent homogeneous mixture in the

TABLE I. Values for the glass transition temperatures T_g and fit parameters A, B, T_0 leading to the VFT and Arrhenius ($T_0 = 0$) curves in Fig. 3. The values of $T_{g\text{-}D}$ and $T_{g\text{-}\alpha}$ are based upon the VFT fits to Debye and α-processes with the criterion $\tau_g(T_g) = 100$ s.

		D-process				α-process				β-process	
Sample	$T_{g\text{-}D}$ [K]	A	B [K]	T_0 [K]	$T_{g\text{-}\alpha}$ [K]	A	B [K]	T_0 [K]	m	A	B [K]
3M3H	...	...	...	...	158.3	−13.6	693	113.9	55.6	−12.5	1150
4M3H	163.7	−15.6	1210	95.1	160.4	−14.9	999	101.4	46.1	−12.5	1290
5M3H	166.4	−16.7	1560	83.0	161.6	−14.6	1050	98.4	42.6	−14.0	1340
6M3H	166.2	−17.9	2050	63.1	156.3	−16.4	1510	74.1	34.9	−14.8	1500
nPOH-4M3H											
x = 0.025	165.5	−15.4	1240	94.5	161.2	−14.2	974	101.1	43.4	−16.2	1940
x = 0.051	164.6	−16.0	1340	90.4	160.4	−14.9	1090	96.1	42.1	−13.6	1440
x = 0.075	164.6	−17.1	1630	79.1	160.4	−13.7	894	103.4	44.1	−16.8	2010
x = 0.098	164.8	−16.9	1590	80.4	160.7	−13.8	938	101.5	43.0	−17.0	1780
x = 0.150	162.8	−17.4	1800	70.1	159.7	−12.7	714	111.0	48.1	−14.1	1530
x = 0.201	160.4	−16.7	1680	70.8	154.4	−16.4	1300	83.6	39.9	−19.5	2370

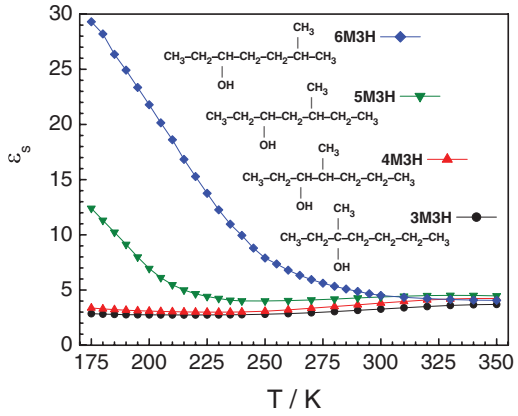

FIG. 4. Temperature dependence of the static dielectric constant, $\varepsilon_s(T)$, for the four isomeric octyl alcohols as identified in the legend: 3M3H, 4M3H, 5M3H, and 6M3H. The graph includes the structures of the isomers.

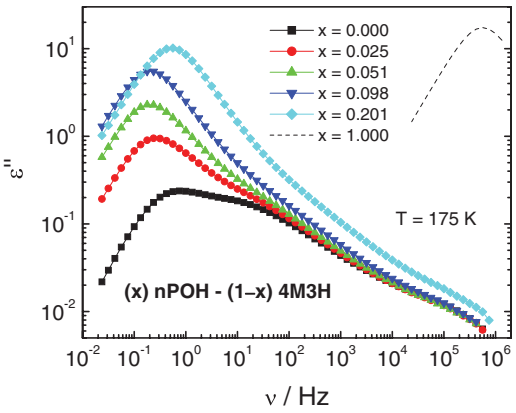

FIG. 6. Dielectric loss spectra of mixtures of nPOH with 4M3H at $T = 175$ K, with the compositions identified in terms of the mole fraction x of nPOH. The loss peak for pure nPOH shown as dashed line is taken from Ref. 5.

temperature range of interest, but above $x = 0.20$ the solution lacks transparency and appears to phase separate. Consequently, only compositions with $x \leq 0.2$ have been studied. The effect of nPOH mole fraction x on the dielectric loss spectrum is indicated in Fig. 6, which focuses on a single temperature of 175 K. Across the composition range of up to 10% of added nPOH, the glass transition temperature is virtually constant (see Table I), while the Debye peak is subject to a slight increase in relaxation time and a dramatic elevation of its amplitude. Only for $x = 0.2$ one can observe a shift of the dynamics towards those of pure nPOH, indicated in Fig. 6 as dashed line.

The activation behavior for the nPOH-4M3H mixture is outlined in Fig. 7, for $x = 0$, 5.1%, 9.8%, and 20%. All cases display a Debye type process as the slowest dielectric mode, as well as a primary (α) and secondary (β) structural relaxation process. As the concentration of nPOH in 4M3H is increased, a more noticeable separation between Debye and α-relaxation can be observed near the glass transition in the relaxation map. The effect of temperature on the static dielectric constants of all nPOH-4M3H mixtures is depicted in Fig. 8. The significant increase in ε_s that originates from the addition of relatively small amounts of nPOH is obviously limited to the lower temperature range near 175 K, and the effect is much smaller already around 250 K. The inset of Fig. 8 indicates that the rise of ε_s versus x observed at $T = 175$ K is much more rapid than what is expected on the basis of an ideal mixing relation with a linear dependence of ε_s on the nPOH mole fraction x.

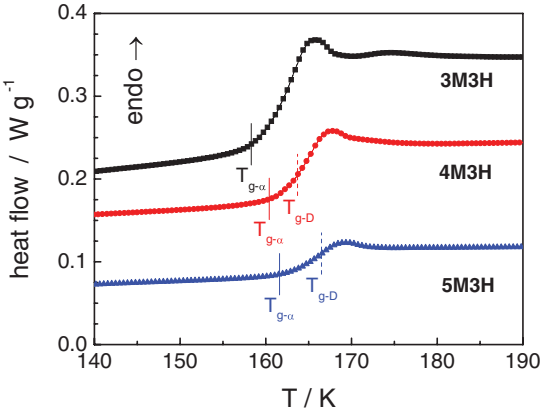

FIG. 5. Differential scanning calorimetry results for three of the isomeric octyl alcohols as labeled. The results are obtained on heating at a rate of 10 K/min, after cooling at the same rate to 130 K. The solid ($T_{g\text{-}\alpha}$) and dashed ($T_{g\text{-}D}$) vertical lines represent the kinetic glass transition temperatures, obtained via the VFT fits using the criterion of the α- and the D-peak time constant reaching $\tau_g = 100$ s, respectively. The onset temperatures derived from the DSC traces yield calorimetric glass transition temperatures of $T_{g,cal} = 159.2$ K (3M3H), 161.6 K (4M3H), and 162.3 K (5M3H).

C. High field dielectric spectra

The field induced effects of this study are reported as the difference between the storage component of permittivity at

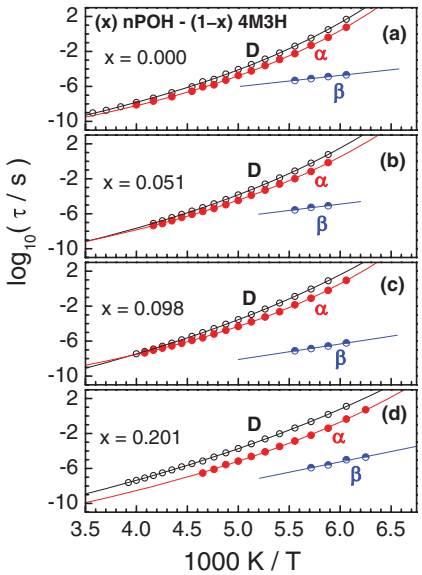

FIG. 7. Activation plot of the time constants τ_D, τ_α, and τ_β for four compositions of mixtures of nPOH with 4M3H. Symbols represent the experimental fit parameter results, while the solid lines are for the VFT fits using the parameters listed in Table I. The different panels are for various nominal mole fractions x of nPOH: (a) $x = 0.000$, (b) $x = 0.051$, (c) $x = 0.098$, and (d) $x = 0.201$.

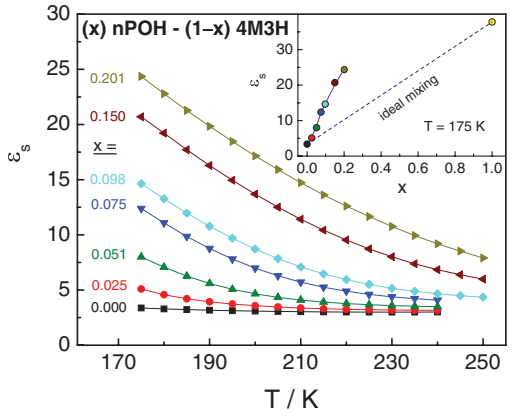

FIG. 8. Temperature dependence of the static dielectric constant, $\varepsilon_s(T)$, for various compositions of mixtures of nPOH with 4M3H, as indicated in terms of the mole fraction x of nPOH. The inset shows the increase of ε_s with mole fraction x at $T = 175$ K, which is much more rapid than the linear interpolation between the pure components included as dashed line.

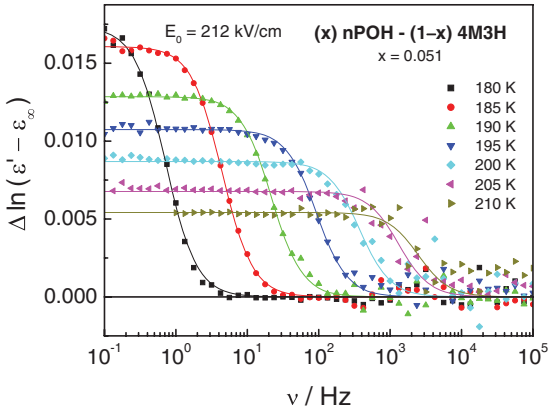

FIG. 10. Field induced relative increase of the non-instantaneous contribution to the permittivity versus frequency, calculated as $\Delta\ln(\varepsilon' - \varepsilon_\infty) \approx (\varepsilon'_{\rm hi} - \varepsilon'_{\rm lo})/(\varepsilon'_{\rm lo} - \varepsilon_\infty)$ for a mixture of nPOH with 4M3H at a mole fraction $x = 0.051$ of nPOH. Here, "hi" and "lo" refer to a field of $E_0 = 212$ kV/cm and $E_0 = 14$ kV/cm, respectively. Different curves are for different temperatures as indicated. Lines are fits according to Eq. (4).

the high field, $\varepsilon'_{\rm hi}$, and its low field counterpart, $\varepsilon'_{\rm lo}$. The low field permittivity is always recorded within the regime of linear response. In the present context, only the relative changes of ε' are relevant, and the instantaneous contribution, ε_∞, is considered field invariant. Therefore, the quantity of interest is given by

$$\Delta\ln(\varepsilon'(\omega) - \varepsilon_\infty) \approx \frac{\varepsilon'_{hi}(\omega) - \varepsilon'_{lo}(\omega)}{\varepsilon'_{lo}(\omega) - \varepsilon_\infty}, \qquad (3)$$

with the approximation in Eq. (3) improving in the limit of very small field induced effects. In the limit of low frequencies, where $\varepsilon'(\omega)$ approaches ε_s, the quantity of Eq. (3) is designated $\Delta\ln(\varepsilon_s - \varepsilon_\infty)$. All $\Delta\ln(\varepsilon' - \varepsilon_\infty)$ results reported below increase quadratically with the amplitude E_0 of the high field, $E(t) = E_0\sin(\omega t)$.

The effect of a high field on the permittivity of 5M3H is shown in terms of $\Delta\ln(\varepsilon' - \varepsilon_\infty)$ in Fig. 9. Although qualitatively similar to a previous high field measurement on the same alcohol,[39] the present overall amplitude of the field effect is somewhat lower, and reductions of ε' seen

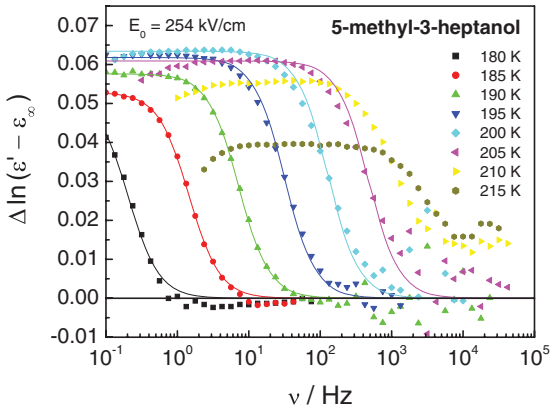

FIG. 9. Field induced relative increase of the non-instantaneous contribution to the permittivity versus frequency, calculated as $\Delta\ln(\varepsilon' - \varepsilon_\infty) \approx (\varepsilon'_{\rm hi} - \varepsilon'_{\rm lo})/(\varepsilon'_{\rm lo} - \varepsilon_\infty)$ for 5M3H. Here, "hi" and "lo" refer to a field of $E_0 = 254$ kV/cm and $E_0 = 14$ kV/cm, respectively. Different curves are for different temperatures as indicated. Lines are fits according to Eq. (4).

earlier at higher frequencies do not appear in the current measurements. The present pattern of the relative increase of $\varepsilon' - \varepsilon_\infty$ can be reproduced at various fields and for separately prepared samples. The advantage of the present experimental approach is the sample thickness of 10 μm (versus 25 μm in the previous[39] case), which reduces sample heating by more than a factor of five. The main feature of Fig. 9 is the field induced increase of the dielectric constant by more than 6%, and the disappearance of this effect for frequencies in excess of the Debye peak position, i.e., $\nu \gg 1/(2\pi\tau_{\rm D})$. The reduction of the field effect at the lowest frequencies is due to dc-conductivity, the failure to reach zero at high frequencies for the higher temperatures is a heating effect from energy absorbed from the field.[42]

Analogous high field experiments on 4M3H and its mixtures with nPOH were performed for fields of $E_0 = 212$ kV/cm. The case of a mole fraction of $x = 0.051$ nPOH in 4M3H is shown in Fig. 10. The overall appearance of the resulting $\Delta\ln(\varepsilon' - \varepsilon_\infty)$ curves follow the pattern of the 5M3H case of Fig. 9. These curves can be fit by the real part of a Debye type function

$$\frac{\varepsilon'_{hi}(\omega) - \varepsilon'_{lo}(\omega)}{\varepsilon'_{lo}(\omega) - \varepsilon_\infty} \approx \frac{\varepsilon_{s-hi} - \varepsilon_{s-lo}}{\varepsilon_{s-lo} - \varepsilon_\infty} \times \frac{1}{1 + \omega^2\tau_T^2}, \qquad (4)$$

where $\varepsilon_{\rm s\text{-}hi}$ and $\varepsilon_{\rm s\text{-}lo}$ are the static dielectric constants at high and low fields, respectively, and $\tau_{\rm T}$ represents the time constant for the transition from zero to the steady state field effect. In this manner, the frequency dependent field effect on ε' can be characterized by its amplitude, $\Delta\ln(\varepsilon_s - \varepsilon_\infty)$, and its transit frequency, $\nu_{\rm T} = 1/(2\pi\tau_{\rm T})$, or its time constant equivalent, $\tau_{\rm T}$. Unfortunately, a theoretical framework for analyzing these results in a more meaningful way is not yet available. The amplitudes of all high field experiments performed at a field of $E_0 = 212$ kV/cm are reported as $\Delta\ln(\varepsilon_s - \varepsilon_\infty)$ in Fig. 11, which includes the two neat octanols 4M3H and 5M3H, and the mixtures of nPOH with 4M3H up to a nPOH mole fraction of $x = 9.8\%$. The transition time constants, $\tau_{\rm T}$, together with the Debye times, $\tau_{\rm D}$, are

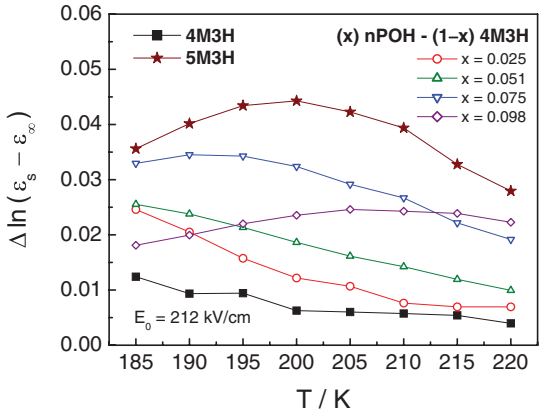

FIG. 11. Field induced relative increase of the non-instantaneous contribution to the dielectric constant versus temperature, calculated as $\Delta\ln(\varepsilon_s - \varepsilon_\infty) \approx (\varepsilon_{s\text{-hi}} - \varepsilon_{s\text{-lo}})/(\varepsilon_{s\text{-lo}} - \varepsilon_\infty)$. Here, "hi" and "lo" refer to a field of $E_0 = 212$ kV/cm and $E_0 = 14$ kV/cm, respectively. Different curves are for different samples as indicated.

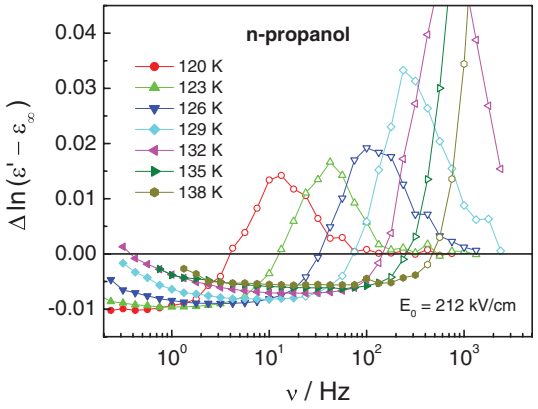

FIG. 13. Field induced relative change of the non-instantaneous contribution to the permittivity versus frequency, calculated as $\Delta\ln(\varepsilon' - \varepsilon_\infty) \approx (\varepsilon'_{hi} - \varepsilon'_{lo})/(\varepsilon'_{lo} - \varepsilon_\infty)$ for nPOH at temperatures between 120 K and 138 K. Here, "hi" and "lo" refer to a high field of $E_0 = 212$ kV/cm and a low field of $E_0 = 14$ kV/cm, respectively. Solid symbols indicate the regime of the static dielectric constant plateau, with $\varepsilon' \approx \varepsilon_s \pm 5\%$.

depicted versus temperature for 4M3H and 5M3H in Fig. 12. For the remaining samples subject to high field experiments, the position of τ_T relative to τ_D is shown as $\log_{10}(\tau_T/\tau_D)$ in the inset of Fig. 12. Regardless of sample and temperature, the relation $\tau_T \approx 2\tau_D$ appears to serve as a good approximation.

For neat nPOH, the effect of a high electric field on ε' differs qualitatively from the above examples. As shown in Fig. 13, a reduction of the dielectric constant is observed in the regime for which permittivity is near its static dielectric constant plateau, i.e., where $\varepsilon' \approx \varepsilon_s \pm 5\%$ (solid symbols). The positive contributions at the higher frequencies originate from shifts in the Debye peak position towards higher frequencies as a result of absorbing energy from the strong electric field.[43] The interesting feature of this result is that the neat liquids 4M3H and nPOH display respective field effects of $+1\%$ and -1% at $E_0 = 212$ kV/cm, whereas their mixtures show more considerable enhancements of the dielectric constant of up to $+3.5\%$ at the same field.

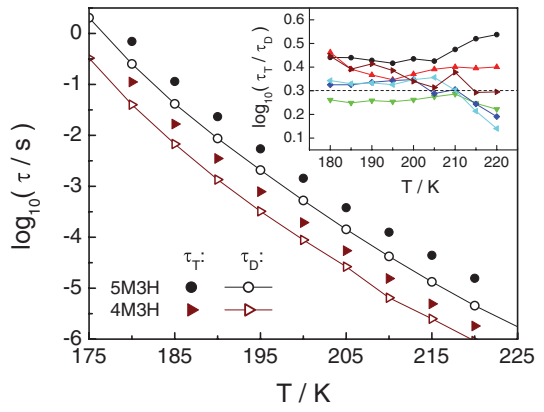

FIG. 12. Solid symbols represent transition time constants, τ_T, of the field induced relative increase of the non-instantaneous contribution to the permittivity versus frequency, obtained by Debye fits to $\Delta\ln(\varepsilon' - \varepsilon_\infty)$ curves such as those shown in Fig. 9. For a comparison, the open symbols are for the linear response Debye process relaxation times, τ_D. The main figure shows τ_T and τ_D for 4M3H and 5M3H, as indicated. The inset depicts the time constant separation, $\log_{10}(\tau_T/\tau_D)$, versus temperature for all samples investigated with high fields: circles – 5M3H, triangles up – $x = 9.8\%$, triangles down – $x = 7.5\%$, diamonds – $x = 5.1\%$, triangles left – $x = 2.5\%$, triangles right – 4M3H, with x representing the nPOH mole fraction of the nPOH-4M3H mixtures.

IV. DISCUSSION

A. Linear response results

The peak assignment generally accepted for typical mono-hydroxy alcohols is for the systems that exhibit a prominent dielectric Debye peak as the lowest frequency dielectric relaxation feature, a faster and much smaller dispersive peak matching the α-relaxation, and possibly a further secondary relaxation at even higher frequencies. In many of the well studied mono-hydroxy alcohols such as *n*-propanol[5,44–46] and 2-ethyl-1-hexanol,[4,47] the amplitude of the Debye peak accounts for 90% or more of the total dielectric relaxation strength. Not all of the octyl alcohols of this study match that behavior, as 3M3H has no Debye peak, the Debye peak of 4M3H is comparable in amplitude to the α-process, and for 5M3H the Debye amplitude is much below 90% of the total $\Delta\varepsilon$ and strongly dependent on temperature. Therefore, it is useful to verify that the peak labeled "α" corresponds to the signature of structural relaxation via DSC results. Fig. 5 compares the kinetic T_g's based on a $\tau_g(T_g) = 100$ s criterion for the Debye type peak and for the lowest frequency dispersive process with the DSC onset temperature. For all three cases, 3M3H, 4M3H, and 5M3H, the peaks labeled "α" in Fig. 3 conform to the onset temperature of the heat capacity step based upon a 10 K/min scan rate, thereby confirming the assignment as primary structural relaxation mode. The kinetic T_g values associated with the Debye peak, $T_{g\text{-}D}$, are significantly higher and thus incompatible with a relevant structural mode.

The nature of the secondary relaxation of the octanol isomers is assessed regarding its Johari-Goldstein (JG) character. A JG type β-relaxation is considered a motional feature intrinsic in the dynamics of glass-forming materials,[14] while other secondary processes could originate from intramolecular degrees of freedom. Although the Coupling Model (CM)

does not capture microscopic details, it provides predictions for the activation behavior of a JG mode that are commonly accepted as indicators for the nature of the secondary process. For the liquid state with $T > T_g$, the CM predicts the following scaling of the JG time constant, τ_β, relative to τ_α and the so-called primitive relaxation time $\tau_c = 2$ ps:[48]

$$(\lg \tau_\beta - \lg \tau_\alpha) = (1 - \beta_{KWW})(\lg \tau_c - \lg \tau_\alpha), \quad (5)$$

where β_{KWW} is the KWW stretching exponent. For the glassy state with $T < T_g$, the following relation for the Arrhenius law parameters of Eq. (1), A and B, is expected on the basis of the CM:[49,50]

$$B = T[\beta_{KWW} \log_{10}(\tau_g / s) + (1 - \beta_{KWW}) \log_{10}(\tau_c/s) - A], \quad (6)$$

where $\tau_g = \tau_\alpha(T_g) = 100$ s. The prediction of the relation given by Eq. (5) is included as stars in the activation map of the octanols, Fig. 3, for $T > T_g$. The logarithmic prefactors, A, and activation parameter, B, from Arrhenius fits to the $\tau_\beta(T)$ data (see Table I) conform to Eq. (6). The agreement of the CM criteria with the observed values for τ_β suggests that the secondary processes of all four octanol isomers are JG type β-relaxations.

The understanding that could emerge from designating the two dispersive (non-Debye) peaks as the "α" and "β" components of structural relaxation is that all four octanols display the generic supercooled liquid behavior, but with an extra slow dielectric Debye process that remains to be detected by experiments that do not probe electrostatic interactions. The case of viscous 3M3H that lacks a Debye peak would then appear as a simple glass-forming liquid in terms of its activation behavior, but its dielectric constant is too small (see Figs. 1 and 4) to be consistent with the uncorrelated reorientation of molecules with the considerable dipole moment of the hydroxyl group. A similar notion holds for all mono-hydroxy alcohols that display a prominent Debye peak: While the dielectric α-process reflects the dynamics of the primary structural relaxation, its small amplitude implies that this loss peak is not equivalent to the correlation decay of the molecular dipole orientation. As a result, the amplitudes of the dielectric peaks require careful consideration.

According to the $\varepsilon_s(T)$ curves in Fig. 4, the dielectric constants and their temperature dependence differ dramatically for these octanol isomers,[51] although the molecular dipole moments and number densities are virtually identical for the four liquids.[34] As recognized already by Dannhauser,[34] it is the orientational correlation of neighboring dipoles that determines the effective squared dipole moment, $g_K\mu^2$, where μ is the dipole moment of the isolated molecule. The statistical mechanical result on how the average cosine of the angle, $\cos\theta$, of z coordinated neighbors affects the effective squared dipole moment is $g_K = 1 + z\langle\cos\theta\rangle$.[52] For a dipolar liquid, the Kirkwood-Fröhlich equation establishes a link between g_K and the dielectric constants in the limit of high (ε_{inf}) and low (ε_s) frequencies,[38]

$$g_K = \frac{9\, k_B T \varepsilon_0 M}{\rho N_A \mu^2} \times \frac{(\varepsilon_s - \varepsilon_{inf})(2\varepsilon_s + \varepsilon_{inf})}{\varepsilon_s (\varepsilon_{inf} + 2)^2}, \quad (7)$$

with N_A being Avogadro's constant, ρ the density, M the molar mass, k_B is Boltzmann's constant, and ε_0 represents the permittivity of vacuum. Usually, ε_{inf} is set to ε_∞ or $1.05 \times n^2$, with n being the refractive index. The variable "ε_{inf}" in Eq. (7) is deliberately distinguished from the usual high frequency limit "ε_∞," as values other than ε_∞ will be used for ε_{inf} in the Kirkwood analysis further below. For mono-hydroxy alcohols, the value of g_K has served as a significant source of structural information,[2,20,34,53–55] as $g_K > 1$ and $g_K < 1$ indicate a preference for parallel and anti-parallel orientation of neighboring dipoles, respectively. The case $g_K = 1$ is usually understood as the absence of dipole correlations, as found for many simple liquids.

Dannhauser[34] has determined $g_K(T)$ for the four octanol isomers of this study, and concluded that $g_K > 1$ and $g_K < 1$ are the consequence of chain and ring like hydrogen-bonded structures, respectively, with their equilibrium constant changing with temperature. Accordingly, $g_K \approx 1$ can originate from a balance of chains and rings, and not necessarily from the lack of orientational correlations.[2] The rationale for the existence of different structures is the systematic change on the –CH3 to –OH group distance along the isomer series, creating different levels of steric hindrance to the formation of open hydrogen-bond chain structures.[34]

A different approach to a systematic variation of the Kirkwood correlation factor is by mixing two mono-hydroxy alcohols, one characterized by $g_K < 1$ and one with $g_K > 1$. The present choice is 4M3H for the component that prefers to form rings in its pure state ($g_K = 0.2$ at $T \approx T_g$), and nPOH for the chain promoting species ($g_K = 3.2$ at $T \approx T_g$). Although the kinetic glass transition temperatures for the two components in their pure states are very different ($T_g = 97$ K for nPOH[56] and $T_g = 160$ K for 4M3H), the mixtures with nPOH mole fraction $x < 0.2$ display very little change regarding the primary structural dynamics. It is also obvious from Fig. 6 that the present mixture of alcohols that are chain (nPOH) and ring (4M3H) dominated in their pure states does not follow the ideal mixing rule regarding τ_D that has been observed for binary aliphatic alcohols with little tendency of either pure component to form rings.[57]

As evident from Figs. 6 and 8, the static dielectric constant changes considerably with composition of the nPOH-4M3H mixture in the present range, $0 \le x \le 0.2$, especially at the lower temperatures. Noteworthy is the observation that ε_s increases more rapidly with nPOH content than what is expected on the basis of an ideal mixing rule, i.e., assuming a linear ε_s-x relation. Actually, the ideal mixing behavior regarding ε_s should be expected only if each hydrogen-bonded structure contains only one component, nPOH or 4M3H. A much more realistic picture is the assumption of a random composition along the chain contour, analogous to random co-polymers. In this case, nPOH within the chain is likely to reduce the steric constraints that prevented extended open chains in the pure 4M3H case, thus giving rise to a strongly positive excess of ε_s relative to the ideal mixing scenario. However, as with the cases of 5M3H and 6M3H in Fig. 4, the increase of ε_s promoted by the addition of nPOH in the mixtures with 4M3H fades as the temperature is increased, see Fig. 8.

B. High field effects

Field induced increases of the dielectric constant of alcohol solutions have been observed by Małecki[58,59] and Piekara,[60] who referred to this feature as "positive saturation effect" and related its occurrence to hydrogen-bonding and the existence of dimers with anti-parallel dipole orientation. More recently, field effects on the dielectric properties of pure 5M3H have been studied using impedance techniques at peak fields of $E_0 = 170$ kV/cm.[39] A significant field induced increase of the dielectric constant was observed, and the field effect disappeared for frequencies exceeding the loss peak position of the Debye process. From those preliminary results, it was concluded that the origin of the dielectric Debye peak is the fluctuation of the end-to-end dipole of chain like structures. The basis for this model is the recognition that the high field shifts the chain/ring equilibrium constant towards the more dipolar chain structures, and that the ring-to-chain conversion involves a time scale close to that of the low field Debye peak.[39]

The results of an improved version of the above mentioned high field experiments on 5M3H are depicted in Fig. 9, which report the field effect as the relative change of the non-instantaneous contribution to ε', see Eq. (3). The main experimental improvements are the extended frequency range and the reduction of field induced sample heating by a factor of >5, achieved by the reduction in sample thickness to 10 μm.[42] As a result, the new curves transition from a low frequency plateau to zero, without the intermediate negative values observed before, thereby conforming to Eq. (4) as phenomenological description. The field induced enhancement of the dielectric constant is explained by the relatively low correlation factor, g_K, suggesting a chain/ring equilibrium constant, $K_{c/r}$, whose value is not far from unity. Accordingly, chain and ring structures have similar free energies and a field of several hundred kV/cm can modify the value of $K_{c/r}$ towards a higher population of the more polar species. The frequency dependence of this field effect then provides information of the time scale involved in the ring-to-chain conversion, τ_T in Eq. (4). From the preliminary data,[39] it was concluded that $\tau_T \approx \tau_D$, suggesting that the Debye process is the signature of end-to-end vector fluctuation of the open chain structures.

A critical test of the above interpretation of the field effect would be the demonstration of a diminished $\varepsilon_s(E)$ sensitivity for the cases $K_{c/r} \ll 1$ and $K_{c/r} \gg 1$. In either limit, a small field induced shift in the free energy of the polar component, i.e., chains, will have little effect of the fraction of chain structures and thus on the value of ε_s. If, instead, the role of the field would be to enlarge the net dipole moments of chains, then the field effect should be more pronounced for liquids with $K_{c/r} \gg 1$ and accordingly high g_K. Evidence for a reduced field effect for the $K_{c/r} \ll 1$ case is compiled in Fig. 11, which shows the magnitude of $\Delta\ln(\varepsilon_s - \varepsilon_\infty)$ for 4M3H, 5M3H, and nPOH-4M3H mixtures at various compositions. The case of pure 4M3H displays the least sensitivity to field, ≈1% at a field of $E_0 = 212$ kV/cm, and it is also the liquid with the most pronounced preference to form ring-structures,[34] consistent with its very low dielectric constant, see Fig. 4. The idea of a diminished field effect for values of $K_{c/r}$ that are sufficiently above or below unity is supported by the nPOH-4M3H mixture results. According to Fig. 11, an increased nPOH mole fraction up to $x = 9.8\%$ leads to a maximum in the magnitude of the field effect. Finally, the effect of a field of $E_0 = 212$ kV/cm on pure nPOH is seen in Fig. 13, which shows no enhancement of ε_s. Instead, the high dielectric constant of nPOH is responsible for the opposite effect: dielectric saturation at a level that is within a factor of two of the effect that is expected on the basis of van Vleck's theory of saturation in dense dipolar liquids.[61] The positive effect observed at higher frequencies is the result of the energy that the Debye loss peak absorbs from the field.[43] The result is that both pure liquids, 4M3H with $g_K \ll 1$ and nPOH with $g_K \gg 1$, show minimal sensitivity of their ε_s to high fields, whereas their mixtures show considerable enhancements of the dielectric constant. These observations support the notion that the high electric field shifts the value of $K_{c/r}$ upward by lowering the free energy of the chains, which leads to a considerable population change only if $K_{c/r}$ is near unity.

The main feature of the high field study is not the capability of shifting the chain/ring equilibrium with an electric field. Rather, it is more important that the experimental results allow us to associate a time scale, τ_T, with the conversion from rings to open chains. When the frequency of the high field impedance measurement exceeds the frequency characterizing that structural transformation, i.e., $\nu > \nu_T = 1/(2\pi\tau_T)$, then the effect of an enhanced dielectric constant will disappear. This effect is clearly borne out by the 5M3H results of Fig. 9, and by the analogous $\Delta\ln(\varepsilon' - \varepsilon_\infty)$ curves for 4M3H and the nPOH-4M3H mixtures (not shown). The values of τ_T are derived via Eq. (4) and display a simple relation to the time constant of the Debye process for all samples, $\tau_T \approx 2\tau_D$. All 54 points included in the inset of Fig. 12 lead to the statistics $\log_{10}(\tau_T/\tau_D) = 0.34 \pm 0.08$, i.e., there is little variation with compound, composition, or temperature. From this proximity of τ_T to τ_D, we conclude that the Debye process is the dielectric signature of the end-to-end vector fluctuation of open chains, a process that will be subject to the same hydrodynamic friction and rotational barriers as the ring/chain transformation. Chains that fluctuate regarding their contour topology can minimize their polarization by a very small end-to-end distance or by an end-to-end dipole moment that is aligned perpendicular to the field direction. This may explain the factor of approximately 2 between τ_T and τ_D.

C. End-to-end dipole fluctuation model

Hydrogen-bonded structures have a long history in the explanation of dielectric relaxation features of mono-hydroxy alcohol and similar liquids.[2,3,36] Models involving end-to-end vector fluctuations analogous to polymer chain dynamics have been proposed by Levin and Feldman[26] and later by Gainaru *et al.*[28] The present work builds upon the recent observation that the time scale of (field induced) conversions of hydrogen-bonded structures matches the dielectric Debye time τ_D,[39] which is considered evidence for understanding the Debye peak as the signature of fluctuations in the net Kirkwood factor g_K. The results from the present much more detailed study

corroborate the understanding of the field effect as a shift of the free energy of open chain structures and the concomitant measurable change if the chain/ring equilibrium constant, $K_{c/r}$, towards favoring the more polar chain configurations and thus raising g_K and ε_s. This process is analogous to a chemical equilibrium between a polar and a non-polar species, which will give rise to a Debye peak whose time scale is governed by the rate constants involved.[62]

It is important to realize that realistic electric field amplitudes will shift the chain/ring equilibrium to an extent that is detectable via changes in $\varepsilon'(\omega)$ only when the free energies of the two hydrogen bonded topologies are similar, i.e., when g_K is near unity. Accordingly, the present high field experiments can determine the time scale involved in a considerable change of the end-to-end distance only for the $g_K \approx 1$ cases. For other alcohols with $g_K \gg 1$, such as nPOH or 2-ethyl-1-hexanol, end-to-end distances will also fluctuate between more extended and more compact structures (yet without persistent ring structures). The latter fluctuation will also give rise to a Debye peak, possibly on longer time scales compared with τ_α due to larger net hydrodynamic volumes. Note that for the above examples for which $\tau_D \approx 2\tau_T$ is observed, the separation of Debye and α-peak covers a range of one decade already, i.e., $2 < \tau_D/\tau_\alpha < 20$ (see below).

Unlike the situation with the normal mode relaxation of polymer chains,[63] a particular structure defined by hydrogen-bond connectivity has a finite lifetime. For rationalizing the dynamics of alcohols, a persistent chain contour length is not required. Bond rotation as well as chain scission and reconnection to other fragments are expected to contribute to the end-to-end dipole fluctuations. For the cases of moderate g_K, a conversion from closed rings to open chains will also contribute. This view is consistent with the inactivity of this Debye mode regarding mechanical and enthalpic modes. However, a change of the chains topology impacts the net orientational correlation along the chain and thus the value of g_K and the polarization.[36] Because end-to-end fluctuations are slow compared with the primary structural relaxation mode and reorientation of the aliphatic tails, effective time-averaging over different environmental conditions occurs and the process is bound to display a Debye character, even for the cases of dispersive structural dynamics.[64]

In standard applications to single component systems, the factor g_K that is meant to gauge the effect of short range correlations is assumed uniform for all processes that contribute to the rise of the permittivity from ε_∞ to ε_s, see Eq. (7). Assuming that the Debye process reflects the end-to-end vector fluctuation of the chains, that the α-process is the molecular reorientation restricted by its hydroxyl group involvement in a chain structure, and that the β-relaxation is a small scale motion within a rigid environment, it seems rather unlikely that a single correlation factor will describe the entire polarization process that spreads over many orders of magnitude in time or frequency. Moreover, the value of g_K is very sensitive to the high frequency baseline, ε_{inf} in Eq. (7). If the dielectric signatures of the primary and secondary relaxation peaks are not subject to the same orientational correlations that govern the Debye process, then ε_{inf} in Eq. (7) should be set closer to $\varepsilon_{inf} = \varepsilon_\infty + \Delta\varepsilon_\alpha + \Delta\varepsilon_\beta$ in order for g_K to reflect the

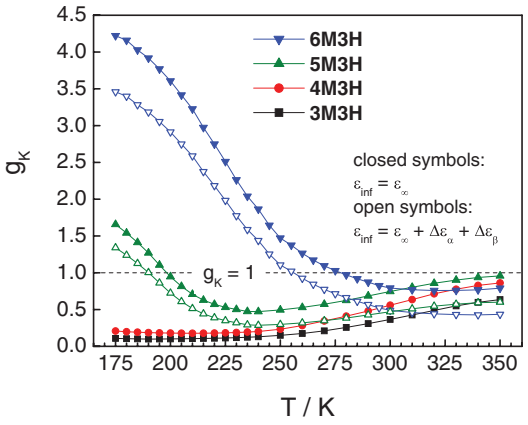

FIG. 14. Kirkwood correlation factors, g_K, versus temperature for the four isomeric octyl alcohols, 3M3H, 4M3H, 5M3H, and 6M3H, as indicated. Solid symbols are based upon using ε_∞ as "infinite frequency" permittivity (ε_{inf}) within the Kirkwood-Fröhlich relation, Eq. (7). Open symbols refer to the calculation using $\varepsilon_{inf} = \varepsilon_\infty + \Delta\varepsilon_\alpha + \Delta\varepsilon_\beta$.

average correlation within structure defined by hydrogen-bond connectivity. This choice for ε_{inf} is compared with the more typical case, $\varepsilon_{inf} = \varepsilon_\infty$, in Fig. 14. The effect of disregarding the α- and β-peaks for the purpose of calculating g_K results in the curves approaching values lower than unity at high temperatures. While the majority of published $g_K(T)$ curves tend to approach unity and thus suggest a lack of correlation at moderately high temperatures,[2,34] there may be many cases in which ring structures dominate at elevated temperatures and $g_K < 1$ characterizes the Debye process. Given the complexity of the dynamics of supercooled alcohols, a frequency dependent correlation factor, $g_K(\omega)$, could turn out more appropriate for assessing orientational correlations within hydrogen-bonded structures.

As seen in Fig. 8, adding nPOH to 4M3H rapidly increases the static dielectric constant of the mixture. In order to assess the concomitant increase of the effective Kirkwood correlation factors of these mixtures, values of $g_{K,eff}$ have been determined using the standard generalization of the Kirkwood-Fröhlich equation for binary systems.[2] The results are compiled graphically in Fig. 15, and they indicate that only $x = 20\%$ nPOH is needed to raise g_K to above 3 from the low value of $g_K \approx 0.25$ of pure 4M3H ($x = 0$).

As mentioned above, the primary structural relaxation of the alcohols leads to a signature within the dielectric spectrum, denoted α-peak, and its time scale matches the mechanical and calorimetric counterparts.[18,19] However, the amplitude of that polarization process is much smaller than what is expected on the basis of the molecular dipole moment.[28] In view of the hydrogen-bonded structures, the explanation is that the hydroxyl group carrying the majority of the dipole moment is engaged in the chain or ring structure and thus highly limited regarding its reorientation on the time scale of the α-process. While structural relaxation of the aliphatic tail of the molecule is possible, translational motion may be more restricted than in a simple liquid. This could be a factor in promoting the low fragilities of these systems, analogous to plastic crystals.[65] The low fragilities and their systematic

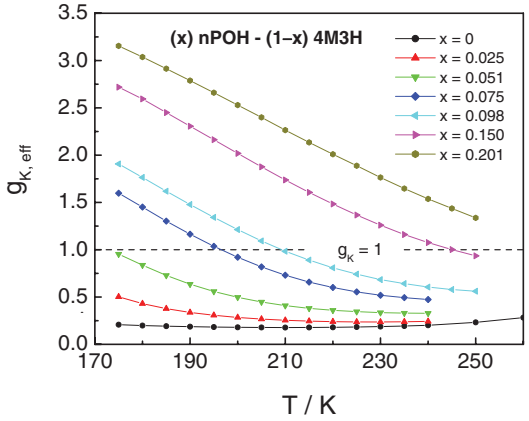

FIG. 15. Effective Kirkwood correlation factors, $g_{K,\,eff}$, versus temperature for various compositions of mixtures of nPOH with 4M3H, as indicated in terms of the mole fraction x of nPOH. All curves are based upon using ε_∞ as "infinite frequency" permittivity in the Kirkwood-Fröhlich relation for binary mixtures.

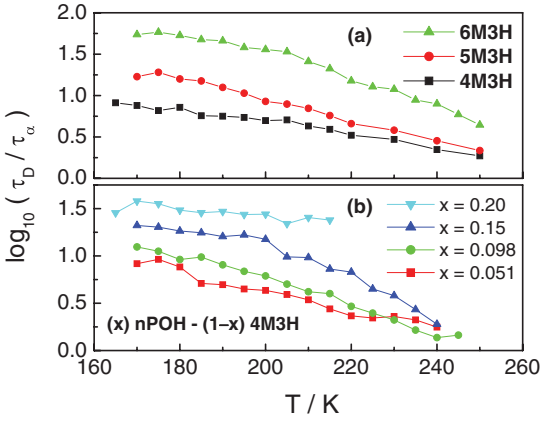

FIG. 17. Spectral separation of Debye and α-peak in terms of $\log_{10}(\tau_D/\tau_\alpha)$ for samples of this study that display a dielectric Debye type process. (a) Results for 4M3H, 5M3H, and 6M3H, as indicated. (b) Results for some of the nPOH-4M3H mixtures identified by their nPOH mole fraction, x.

variation with $-CH_3$ to $-OH$ distance are depicted for the isomeric octyl alcohol series in Fig. 16.

Finally, we ask what properties govern the spectral position of the Debye peak relative to that of the α-process. It is easily envisioned that the end-to-end vector fluctuation is a quasi-hydrodynamic problem and thus under the control of the viscosity of the liquid and the average chain length. As an approximation, this feature of $\tau_D(T)$ roughly following $\eta(T)$ or $\tau_\alpha(T)$ can be observed for numerous alcohols that display a Debye peak associated with supramolecular structures. However, a closer inspection reveals that the spectral separation is far from being independent of temperature or viscosity, and the ratios τ_D/τ_α range from 2 to 2000 in pure systems.[47] For the cases of this study, Fig. 17 compiles the spectral separations of Debye and α-peak in terms of $\log_{10}(\tau_D/\tau_\alpha)$ versus temperature. Qualitatively, these curves resemble the trends of the static dielectric constant, ε_s, or correlation factor, g_K, versus material and temperature. A possible link between ε_s or g_K and τ_D/τ_α could be that the reduction in g_K is a result of an increased barrier for bond rotation through steric hindrance

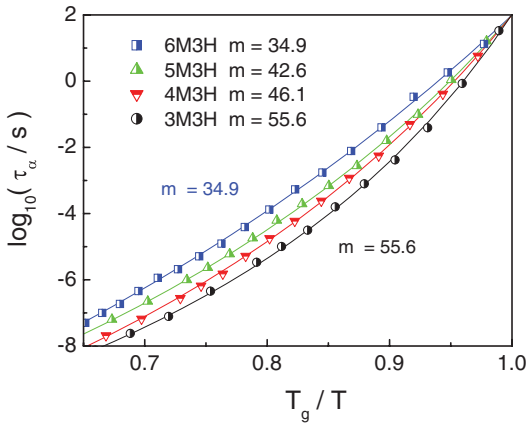

FIG. 16. Angell plot of the characteristic (HN) relaxation time of the α-process of 3M3H, 4M3H, 5M3H, and 6M3H. The symbols identify different octyl alcohols as indicated. The solid lines represent the VFT fits for each liquid using Eq. (1) with the parameters listed in Table I.

(reduced chain flexibility) and possibly the average chain lengths becoming shorter (diminished coordination number z) as the structural preference is shifted towards rings by temperature or composition, leading to a reduction of the τ_D-τ_α separation. Supportive of this notion is that high g_K cases such as n-propanol and 2-ethyl-1-hexanol have $\log_{10}(\tau_D/\tau_\alpha)$ values of 2.2 and 3.3,[5,47] respectively, i.e., beyond the values of 6M3H in Fig. 17.

V. SUMMARY AND CONCLUSIONS

Two series of samples have been studied, in which the Kirkwood correlation factor, g_K, varies systematically from below to above unity. For the isomeric octanols, it is the distance between methyl and hydroxyl group along the carbon backbone that controls g_K. For the mixtures with varying n-propanol content in 4-methyl-3-heptanol, it is the composition that changes the value of g_K. The change from $g_K < 1$ to $g_K > 1$ is understood to reflect the change from compact ring-like to open chain-like structures as the majority type of hydrogen-bonded topology. For both series, the activation behavior of the Debye, the α-, and the β-processes, as well as their amplitudes have been characterized in the linear response regime.

The high-field dielectric experiments illustrate that those systems with g_K near unity are particularly sensitive to the field amplitude, with the effect of a high field being an increase of the static dielectric constant. The explanation of this effect is that a similar population of rings and chains indicates near equal free energies of the two structures, implying that even a moderately high electric field is capable of shifting the equilibrium constant towards the more polar species, thereby favoring chains over rings. The main result, however, is derived from the frequency dependence of the field induced increase of $\varepsilon'(\omega)$. From this frequency dependence, we conclude that the time involved in the field-induced structural change is twice the time constant of the Debye process. This is understood as strong support for the previously reported model in which the dielectric Debye

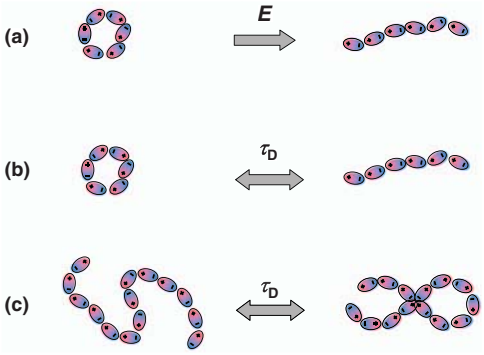

FIG. 18. Pictorial summary of the hydrogen bonded structures and the fluctuations involved: (a) high fields shift population towards more chains, (b) involving a ring/chain conversion that is seen to occur on the time scale of the Debye peak, and (c) implying by analogy that end-to-end distance fluctuations of chains are at the origin of the Debye process. This cartoon depicts only the dipoles along the chain contour (with all alkyl groups omitted), and is not meant to imply long lived connectivity.

peak is viewed as fluctuation of the end-to-end vector of hydrogen-bonded topologies. A pictorial representation of the structures and fluctuations involved is provided in Fig. 18, where (a) indicates the field induced shift of the equilibrium constant towards more chain like structures, (b) represents the observation that ring/chain conversions occur on the Debye process time scale, and (c) is meant to reflect that the Debye process is understood as the signature of end-to-end vector fluctuations of hydrogen bonded structures, even in the case where no rings are formed. This dipolar mode would originate from fluctuations of the chain contour within the viscous environment, but due to the finite lifetime of chain connectivity, end-to-end dipole fluctuations will also be aided by chain scission and reconnection processes. Viewing the chain contour fluctuation as a quasi-hydrodynamic process explains that the Debye time scale tracks the viscosity and the primary structural relaxation time to some extent. The observed correlation between the ratio τ_D/τ_α and $\Delta\varepsilon_D$ suggests that the spectral separation between Debye and α-process is a matter of the chain length or flexibility, both being diminished as the system is driven to a higher population of ring-like structures. Accordingly, situations involving extended open chains will favor a large separation between Debye and α-peak.

In this model of mono-hydroxy alcohol dynamics, the dielectric signature of primary structural relaxation is assumed to originate from the alkyl-tail dynamics, with some coupling to the hydroxyl dipole, especially its component perpendicular to the contour of hydrogen bond connectivity. It seems very unlikely that all three modes, Debye, α, and β, are subject to the same Kirkwood correlation factor, g_K. As an approximation to separating the value of g_K that is associated with dipole orientations within the hydrogen-bonded structures, we use $\varepsilon_{inf} = \varepsilon_\infty + \Delta\varepsilon_\alpha + \Delta\varepsilon_\beta$ as high frequency baseline in the Kirkwood-Fröhlich equations, leading to $g_K < 1$ instead of $g_K \approx 1$ at elevated temperatures. A more quantitative interpretation of g_K may require a refined approach with frequency dependent correlation factor.

ACKNOWLEDGMENTS

This material is based upon work supported by the National Science Foundation (NSF) under Grant No. CHE 1026124 and by L'Agence Nationale de la Rechereche under Grant No. ANR-10-BLAN-0821 (International Collaboration in Chemistry).

[1]F. X. Powell and D. R. Lide, J. Chem. Phys. **42**, 4201 (1965).
[2]C. J. F. Böttcher, *Theory of Electric Polarization* (Elsevier, Amsterdam, 1973), Vol. 1.
[3]C. J. F. Böttcher and P. Bordewijk, *Theory of Electric Polarization* (Elsevier, Amsterdam, 1978), Vol. 2.
[4]S. S. N. Murthy, J. Phys. Chem. **100**, 8508 (1996).
[5]C. Hansen, F. Stickel, T. Berger, R. Richert, and E. W. Fischer, J. Chem. Phys. **107**, 1086 (1997).
[6]C. A. Angell, K. L. Ngai, G. B. McKenna, P. F. McMillan, and S. W. Martin, J. Appl. Phys. **88**, 3113 (2000).
[7]*Broadband Dielectric Spectroscopy*, edited by F. Kremer and A. Schönhals (Springer, Berlin, 2003).
[8]M. D. Ediger, C. A. Angell, and S. R. Nagel, J. Phys. Chem. **100**, 13200 (1996).
[9]R. Kohlrausch, Pogg. Ann. Phys. Chem. **91**, 179 (1854).
[10]G. Williams and D. C. Watts, Trans. Faraday Soc. **66**, 80 (1970).
[11]H. Vogel, Phys. Z. **22**, 645 (1921).
[12]G. S. Fulcher, J. Am. Ceram. Soc. **8**, 339 (1925).
[13]G. Tammann and W. Hesse, Z. Anorg. Allg. Chem. **156**, 245 (1926).
[14]G. P. Johari and M. Goldstein, J. Chem. Phys. **53**, 2372 (1970).
[15]S. S. N. Murthy and S. K. Nayak, J. Chem. Phys. **99**, 5362 (1993).
[16]L.-M. Wang and R. Richert, J. Phys. Chem. B **109**, 11091 (2005).
[17]T. A. Litovitz and G. E. McDuffie, J. Chem. Phys. **39**, 729 (1963).
[18]B. Jakobsen, C. Maggi, T. Christensen, and J. C. Dyre, J. Chem. Phys. **129**, 184502 (2008).
[19]H. Huth, L.-M. Wang, C. Schick, and R. Richert, J. Chem. Phys. **126**, 104503 (2007).
[20]S. S. N. Murthy and M. Tyagi, J. Chem. Phys. **117**, 3837 (2002).
[21]L.-M. Wang, Y. Tian, R. Liu, and R. Richert, J. Chem. Phys. **128**, 084503 (2008).
[22]C. Lederle, W. Hiller, C. Gainaru, and R. Böhmer, J. Chem. Phys. **134**, 064512 (2011).
[23]S. Schildmann, A. Reiser, R. Gainaru, C. Gainaru, and R. Böhmer, J. Chem. Phys. **135**, 174511 (2011).
[24]M. Preuß, C. Gainaru, T. Hecksher, S. Bauer, J. C. Dyre, R. Richert, and R. Böhmer, J. Chem. Phys. **137**, 144502 (2012).
[25]F. X. Hassion and R. H. Cole, J. Chem. Phys. **23**, 1756 (1955).
[26]V. V. Levin and Y. D. Feldman, Chem. Phys. Lett. **87**, 162 (1982).
[27]U. Kaatze, R. Behrends, and R. Pottel, J. Non-Cryst. Solids **305**, 19 (2002).
[28]C. Gainaru, R. Meier, S. Schildmann, C. Lederle, W. Hiller, E. A. Rössler, and R. Böhmer, Phys. Rev. Lett. **105**, 258303 (2010).
[29]N. O. Birge, Phys. Rev. B **34**, 1631 (1986).
[30]D. W. Davidson, Can. J. Chem. **39**, 2139 (1961).
[31]E. Ikada, J. Phys. Chem. **75**, 1240 (1971).
[32]G. P. Johari, O. E. Kalinovskaya, and J. K. Vij, J. Chem. Phys. **114**, 4634 (2001).
[33]O. E. Kalinovskaya, J. K. Vij, and G. P. Johari, J. Phys. Chem. A **105**, 5061 (2001).
[34]W. Dannhauser, J. Chem. Phys. **48**, 1911 (1968).
[35]J. Crossley, L. Glasser, and C. P. Smyth, J. Chem. Phys. **55**, 2197 (1971).
[36]C. Brot, J. Mol. Struct. **250**, 253 (1991).
[37]W. Dannhauser, J. Chem. Phys. **48**, 1918 (1968).
[38]H. Fröhlich, *Theory of Dielectrics* (Clarendon, Oxford, 1958).
[39]L. P. Singh and R. Richert, Phys. Rev. Lett. **109**, 167802 (2012).
[40]S. Havriliak and S. Negami, Polymer **8**, 161 (1967).
[41]S. Bauer, K. Burlafinger, C. Gainaru, P. Lunkenheimer, W. Hiller, A. Loidl, and R. Böhmer, J. Chem. Phys. **138**, 094505 (2013).
[42]A. Khalife, U. Pathak, and R. Richert, Eur. Phys. J. B **83**, 429 (2011).
[43]W. Huang and R. Richert, J. Chem. Phys. **130**, 194509 (2009).
[44]D. W. Davidson and R. H. Cole, J. Chem. Phys. **19**, 1484 (1951).
[45]R. H. Cole and D. W. Davidson, J. Chem. Phys. **20**, 1389 (1952).
[46]A. Kudlik, C. Tschirwitz, S. Benkhof, T. Blochowicz, and E. Rössler, Europhys. Lett. **40**, 649 (1997).
[47]L.-M. Wang and R. Richert, J. Chem. Phys. **121**, 11170 (2004).

[48]K. L. Ngai and M. Paluch, J. Chem. Phys. **120**, 857 (2004).
[49]K. L. Ngai and S. Capaccioli, Phys. Rev. E **69**, 031501 (2004).
[50]S. Capaccioli and K. L. Ngai, J. Phys. Chem. B **109**, 9727 (2005).
[51]G. P. Johari, J. Chem. Phys. **138**, 154503 (2013).
[52]J. G. Kirkwood, J. Chem. Phys. **7**, 911 (1939).
[53]P. Bordewijk, F. Gransch, and C. J. F. Böttcher, J. Phys. Chem. **73**, 3255 (1969).
[54]P. Petong, R. Pottel, and U. Kaatze, J. Phys. Chem. A **103**, 6114 (1999).
[55]U. Kaatze, R. Behrends, and K. von Roden, J. Chem. Phys. **133**, 094508 (2010).
[56]R. Richert and C. A. Angell, J. Chem. Phys. **108**, 9016 (1998).
[57]L.-M. Wang and R. Richert, J. Phys. Chem. B **109**, 8767 (2005).
[58]J. Małecki, J. Chem. Phys. **36**, 2144 (1962).
[59]J. Małecki, J. Chem. Phys. **43**, 1351 (1965).
[60]A. Piekara, J. Chem. Phys. **36**, 2145 (1962).
[61]J. H. van Vleck, J. Chem. Phys. **5**, 556 (1937).
[62]G. Williams, Adv. Mol. Relax. Processes **1**, 409 (1970).
[63]C. M. Roland and C. A. Bero, Macromolecules **29**, 7521 (1996).
[64]J. E. Anderson and R. Ullman, J. Chem. Phys. **47**, 2178 (1967).
[65]R. Brand, P. Lunkenheimer, and A. Loidl, J. Chem. Phys. **116**, 10386 (2002).